1731.

Invited Paper

Silicon photonics non-resonant wavelength filters: comparison between AWGs, echelle gratings and cascaded Mach-Zehnder filters

Wim Bogaerts[a,b,c], Shibnath Pathak[a,b], Alfonso Ruocco[a,b], Sarvagya Dwivedi[a,b]

[a] Photonics Research Group ,Ghent University - imec, Department of Information Technology, Sint-Pietersnieuwstraat 41, 9000 Gent, Belgium

[b] Center for Nano- and Biophotonics, Sint-Pietersnieuwstraat 41, 9000 Gent, Belgium

[c] now also with Luceda Photonics, Noordlaan 21, 9200 Dendermonde, Belgium

ABSTRACT

We present a comparison of different silicon photonics-based wavelength filters for different design criteria (e.g. channel spacing, number of channels, ...) and different performance metrics (e.g. insertion loss or crosstalk). In this paper we compare only non-resonant filters, or finite-impulse response (FIR) filters, such as Arrayed Waveguide Gratings, Echelle Gratings and higher-order cascades of Mach-Zehnder filters. We derive the strengths and weaknesses from their operational principles and confirm those with experimental data from fabricated devices and extrapolated simulations.

Keywords: Silicon Photonics, Arrayed Waveguide Gratings, Echelle Gratings, Mach-Zehnder Interferometer, Wavelength Filter, Wavelength Division Multiplexing

1. INTRODUCTION

Silicon photonics is becoming a technology of choice to build photonic integrated circuits for diverse applications in optical communications,[1] sensing[2,3]and microwave signal processing.[4] The key strength of silicon photonics, compared to other photonic integration technologies such as *silica on silicon*, *III-V semiconductors* or *Lithium niobate* is the potential integration density and the manufacturing infrastructure. Silicon photonics, using silicon as a base material, is compatible with fabrication processes and tools used for the large-scale manufacturing of CMOS circuitry. Over the past decade, several R&D pilot lineas and even industrial fabs have demonstrated a silicon photonics fabrication flow, with the first products on the market.[5] The use of proven mass-fabrication technologies gives silicon photonics a growth potential for high-volume, low-cost applications.

The second key advantage of silicon photonics is the integration scale. Because of the high refractive index contrast, silicon photonic waveguides can have submicrometer cross-section dimensions, and can guide light in bends of only a few micrometer radius. Because of this, many more components can be integrated on the same chip, compared to other, low contrast, integration technologies. Also, several silicon photonics technology platforms now support active electro-optic modulators and detectors.[6,7]

One of the key functionalities required for many applications of photonic integrated circuits, is the use of wavelength filtering.[8] the optical spectrum covers a huge wavelength range, and even when confined within the useful band of 'standard' silicon photonics (using a waveguide core of 200-400nm thickness), the wavelength range can still span from 1200nm to 2500nm, or over 100THz. Such a wavelength range can contain a lot of information, be it as a carrier of communication signals, or information that can be useful for sensing.

Optical communication can benefit of this huge bandwidth through *wavelength division multiplexing* (WDM), where individual high-speed signals are modulated on different wavelength carriers. This can range from coarse WDM with 4 widely spaced channels, to ultra-dense WDM with over thousand closely packed wavelength channels. To effectively multiplex and demultiplex these communication channels, good wavelength filters are required, with sufficiently low insertion loss and a high rejection ratio of the other communication channels.

Further author information: (Send correspondence to W.B.)
W.B.: E-mail: wim.bogaerts@intec.ugent.be, Telephone: +32 9 264 3324

Integrated Optics: Devices, Materials, and Technologies XIX, edited by Jean-Emmanuel Broquin, Gualtiero Nunzi Conti, Proc. of SPIE Vol. 9365, 93650H · © 2015 SPIE
CCC code: 0277-786X/15/$18 · doi: 10.1117/12.2082785

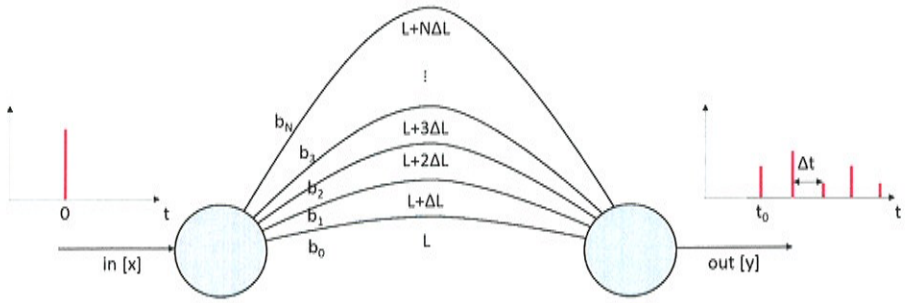

Figure 1. Finite Impulse response filter based on constant delay lines.

Also, wavelength filters can be very useful for sensing applications. Many optical sensors rely on spectral information. This can be a wavelength shift that relates to a specific quantity (e.g. a concentration of biomarkers in a biosensor, or strain in a fiber Bragg grating sensor), or it can be spectroscopic information, such as spectral fingerprints of gases and complex molecules. The requirements for these applications can differ significantly from those of WDM communications.

There are different techniques to make wavelength filters, but almost all rely on interference of two of more light paths. In this paper, we will discuss different implementations of *finite impulse response* (FIR) filters. These filters are based on a finite set of interfering *optical delay lines* in a feed-forward architecture. The main examples of such filters in an integrated circuit include *Mach-Zehnder interferometers* (MZI),[9,10] *arrayed waveguide gratings* (AWG) and echelle gratings.

In contrast to FIR filters, it is also possible to make *infinite impulse response* (IIR) filters in a PIC. These are based on feed-back mechanisms, with optical delay paths coupling back on itself. This will cause multiple self-interference of the light, which leads to resonances. The feedback cavity can be based on a travelling wave, such as in *ring resonators*, or on a standing wave, such as a *Fabry-Perot* cavity. IIR wavelength filters have the significant advantage (compared to FIR filters) that they use the same delay line multiple times. Therefore, they have less problems in matching the lengths of the delays, and the device footprint is usually more compact. However, a key drawback of resonant filters is that the multiple roundtrips also introduce a higher optical peak power in the filter. Therefore, IIR filters can suffer from nonlinear effects, even at low power.[11]

In this paper we will discuss different implementations of FIR filters in silicon photonics. Even though they are based on the same principle of multiple interference paths, the different implementations have their own strengths and weaknesses. In the next section we discuss the operational principles of the different FIR filter types, and identify their strengths and weaknesses. In section 4 we compare the different filter types, as implemented in silicon photonics, against different performance metrics, such as insertion loss, crosstalk, footprint, etc...

2. FIR WAVELENGTH FILTERS

Interferometric FIR wavelength filters are based on optical delay lines. The unfiltered light is split over two or more paths with a different optical path length, and the different contributions are recombined. This is illustrated in Fig. 1. An input impulse is split over the multiple delay lines, and at the output this results in a finite series of impulses, one for each delay lines.

If the path difference between the delay lines is a constant ΔL, the time difference between the impulses is $\Delta t = \Delta L.n_g/c$, with n_g the group velocity of the pulses.

If we ignore the common delay t_0, the output $y(t)$ can be written as a function of the input $x(t)$:

$$y(t) = b_0x(t) + b_1x(t - \Delta t) + b_2x(t - 2.\Delta t) + ... + b_Nx(t - N.\Delta t) \quad (1)$$

In the **Z**-domain we can write this as a polynomial expansion:

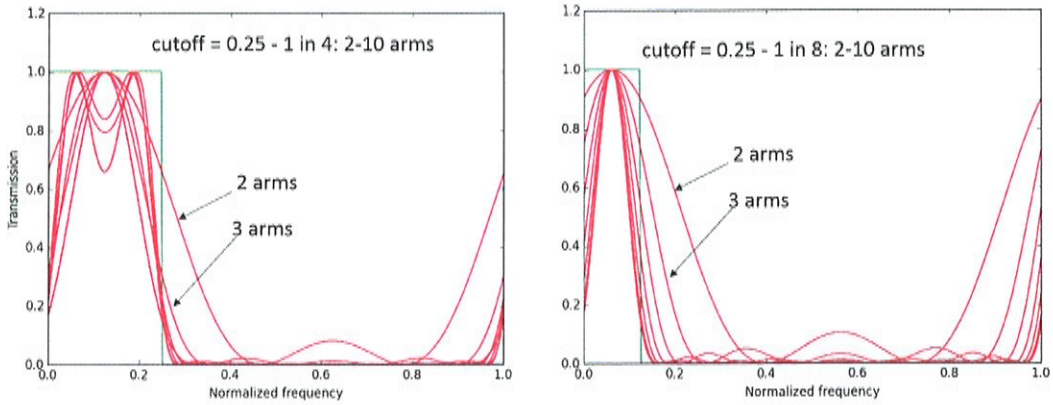

Figure 2. Normalized frequency [f/FSR] response of a FIR bandpass filter with coefficients b_i generated from a truncated Taylor expansion. (a) A 4-channel filter (cutoff=0.25), and (b) an 8-channel fiulter (cutoff=0.125). When we increase the number of arms, we see an improved approximation of the box-like bandpass filter, but for the 8-channel filter we need more arms.

$$\begin{aligned} y[z] &= b_0 + b_1 z + b_2 z^2 + ... + b_N z^N \\ &= (z - q_1)(z - q_2)...(z - q_N) \end{aligned} \tag{2}$$

with q_i the *zeros* of the filter.

In contrast, IIR filters have feedback loop, which results in an impulse response which never completely dies out. In the **Z**-domain this translates into a series of zeros and poles.

In the frequency (or wavelength) domain, the repeating pattern of pulses will also result in a periodic response, with a *free spectral range* (FSR) equal to

$$\begin{aligned} FSR[Hz] &= \frac{1}{\Delta t} = \frac{c}{n_g \Delta L} \\ FSR[nm] &= \frac{\lambda_0^2}{n_g \Delta L} \end{aligned} \tag{3}$$

around a central operating wavelength λ_0.

In the wavelength domain, we can see that the optical delay lines introduce a wavelength dependent phase shift $\Delta\phi(\lambda) = 2\pi n_{eff}(\lambda)\Delta L/\lambda$. When the optical path length difference $n_eff\Delta L$ is exactly a whole number m of wavelengths, the phase difference $\Delta\phi$ between contributions is a multiple of 2π, and they will constructively interfere. Otherwise we will get only partial constructive interfere. When the coefficients of the delay lines are properly chosen, all contributions will add up for the desired wavelength channel $\Delta\lambda$, resulting in a high transmission, while outside that channel they will cancel out, resulting in a low transmission.

Note that the absolute filter wavelength depends on the effective index n_{eff} of the delay line, while the channel bandwidth and the free spectral range, depends on the group index n_g, which includes the wavelength dependence of n_{eff}. In highly dispersive silicon waveguides, the group index can be significantly larger than the effective index.[12]

The narrower the wavelength channel $\Delta\lambda$ with respect to the FSR, the more delay lines will be needed to obtain a well-defined bandpass filter. This is illustrated in Fig. 2, where we approximate a box-shaped

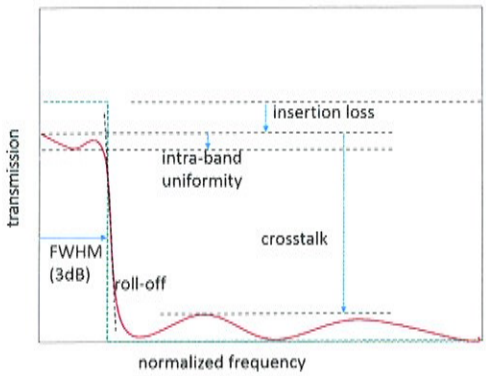

Figure 3. Performance metrics of a wavelength filter. The frequency/wavelength is normalized against a full FSR.

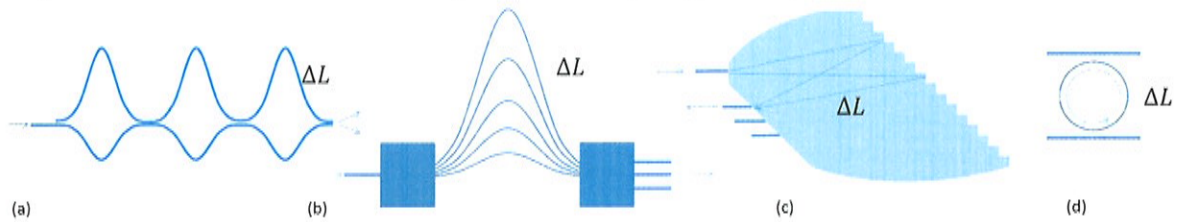

Figure 4. Different implementations of optical filters based on delay lines. (a) a Mach-Zehnder lattice filter, (b) an Arrayed Waveguide Grating (AWG), (c) an echelle grating and (d) a Ring resonator. (a-c) are finite impulse response filters, consisting only of feed-forward delay lines. The ring resonator (d) introduces a feed-back loop, making an infinite-impulse-response filter.

filter response using an increasing number of arms. We see that for a filter which selects one channel out of 4 ($\Delta\lambda/FSR = 0.25$) we already get a good approximation of the desired filter characteristic. However, for the 1-in-8 filter ($\Delta\lambda/FSR = 0.125$) we don't yet obtain a rectangular profile with 10 arms. As a general rule we can say that for n channels, at least $N > 2.n$ delay lines are needed, even with perfect control of the coefficients b_i.

The filter coefficients we used for Fig. 2 were not ideal for a box-like filter. Better coefficients can be calculated based on techniques used in digital filter synthesis, to define *Butterworth*, *Chebyshev* , *Elliptical* or other filter profiles with specific objective functions such as *roll-off* and *crosstalk*.

The performance of a channel filter can be measured by different metrics, which are illustrated in Fig. 3. The bandwidth of a channel is usually expressed as the full-width-half-maximum (FWHM) or 3dB bandwidth. However, often also the 1dB bandwidth and 10dB bandwidth are used. The ratio between the latter two is often used to describe the *roll-off* of the filter. The closer the 1dB/10dB bandwidth ratio is to 1, the more the filter approaches a box-like edge. The *crosstalk* indicates the maximum power collected from outside the channel, and the *insertion loss* indicates the transmission efficiency of the wavelength inside the channel.

3. SILICON PHOTONIC WAVELENGTH FILTERS

Different delay-based filters are illustrated in Fig. 4. A *Mach-Zehnder interferometer* (MZI) splits the light over two arms, effectively introducing a single delay stage, and these can be cascaded to multiple delay stages. An *arrayed waveguide grating* (AWG) distributed light over many delay lines using a *star coupler*, and an *echelle grating* implements the optical delays by positioning reflecting facets at different distances.

The key differences between the filters is how the light is distributed over the different delays and how the contributions are recombined, i.e. the b_i coefficients. As we will discuss further, MZI lattice filters allow, in principle, better control of the b_i coefficients than an AWG or echelle grating. In actual waveguides, the actual

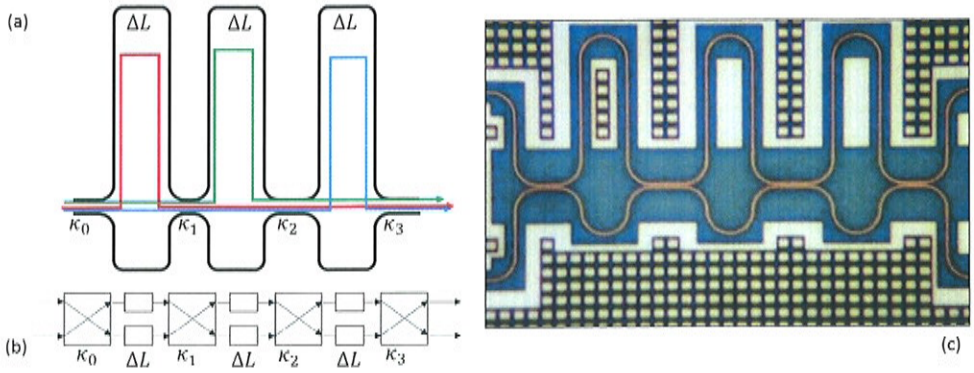

Figure 5. Mach-Zehnder lattice filter. (a) implementation of a 3-stage lattice filters. The first-order delay consists of contributions of 3 different paths through the filter, (b) schematic filter representation, indicating the coupling stages, (c) fabricated device.

phase and amplitude of each b_i contribution depends on the exact geometric definition of the delay, as well as the optical properties of the medium in which the delay is implemented. And this is where the challenges of silicon photonics FIR filters lie.

Silicon photonic waveguides are typically quite *dispersive*. This means that the optical phase delay, and even the group delay, is not constant over a wide wavelength range. This is not necessarily a problem for filters that operate in a narrow wavelength band, but for filters that have to span a broad spectrum, the dispersion could become a problem.

Also, the high refractive index contrast of silicon waveguides makes them very sensitive to small geometry variations, or changes in temperature. This means that the exact optical length of each delay line cannot be precisely controlled.[13] When multiple lines with a supposedly identical delay are used, the *phase errors* will manifest as a higher insertion loss and a higher crosstalk. It is evident that the effect of these stochastic errors increases with longer delay lines, and is strongly dependent on the quality of the fabrication technology. Also, global changes in waveguide geometry (linewidth and thickness) or environmental conditions (temperature) could cause a drift of the filter response.

3.1 MZI Lattice Filters

A simple MZI is a 2×2 filter with a single delay path. By concatenating MZI filters it is possible to create multiple delay paths, as shown in Fig. 5b.[9,10] By routing the light through multiple coupling stages there are now many combinations of optical delays that all combine at the output in different proportions. Also, there are different combinations of paths that lead to the same delay length, as shown in Fig. 5. It is the exact balance between these delays that dictates the filter response, and this is controlled by the coupling ratios of the directional couplers. Such a filter architecture is called a *lattice filter*, and it is commonplace in analog and digital filter banks.

Adding more stages can increase the performance of the filter, but the phase errors in the delay lines will accumulate, and uncertainties in the coupling coefficients will start to deteriorate the performance. While lattice filters usually have two inputs and two outputs, it is possible to cascade multiple filters into a $2 \times N$ filter bank.[14]

3.2 Arrayed Waveguide Gratings

Arrayed waveguide gratings are another mechanism to implement the interference of multiple delay lines.[15] The principle is illustrated in Fig. 6. Incoming light is distributed over many delay lines in a *star coupler*. The individual contributions are then recombined in a second star coupler. However, the recombination mechanism is significantly different from an MZI lattice filter.

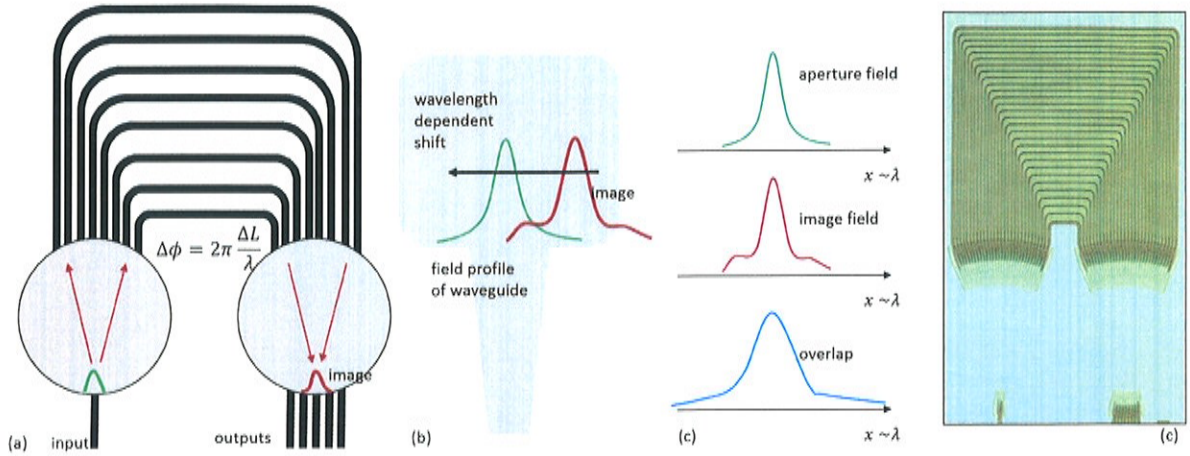

Figure 6. Arrayed Waveguide Gratings. (a) operation principle, (b) Shift of the projected image with wavelength, (c) The overlap of image field profile with the aperture mode gives rise to a wider wavelength response (d) fabricated device.[8]

The star couplers function as an imaging system. When all the contributions of the delay lines are in phase, the field profile of the input aperture is imaged in the plane of the output apertures. The quality of that image depends on the number of contributions (delay lines), but it is never perfect. When the wavelength changes, there will be a constant phase difference between every two arms, and this will tilt the phase front in the output star coupler. This, in turn, will shift the image. Therefore, there is a one-of-one mapping of the position in the image plane to the wavelength within a single FSR. The mode-to-mode response of input to output is determined by the overlap of the image field profile with the mode profile of the output aperture. As shown in Fig. 6c, the imaging and resulting overlap broadens the wavelength response of the filter, to approximately twice the bandwidth. A consequence of this is that an AWG which need to select 1 channel of out N, needs about twice the number of arms than an equivalent MZI lattice filter.

Also, the shifting overlap of the image and the aperture mode, which can be mathematically described as a convolution in the wavelength domain, will smoothen the wavelength response. This makes it difficult to create a box-like band-pass filter in the AWG. This can be compensated by tailoring the aperture field profiles of input and output to create a sharper response: for instance, by including a broader waveguide section (a multimode interferometer) we can obtain a broader, more uniform pass band.[16–18] This, however, comes at the expense of insertion loss. Modifying the coefficients b_i of the individual arms is less straightforward: the amplitudes are largely determined by the far-field profile of the input aperture. However, it is possible to make non-uniform star couplers, but this complicates the control of the relative phases between the arms.[19]

An advantage of the AWG is that the imaging principle makes it possible to create a wavelength demultiplexer, instead of a single channel filter. When positioning multiple waveguide apertures in the output star coupler, different wavelengths will be coupled to different output waveguides. However, the channels will have an uneven insertion loss. The transmission from the center input to the center output is highest, while the transmission between an input and an output both at the edge of the star coupler (or the edge of the FSR in the spectrum) could be 3-6dB lower. A way to overcome this is increase the number of channels within the FSR but not use the outer channels. This requires additional delay lines.[20]

Also, an AWG is not confined to a regular wavelength grid: the output waveguides can be freely positioned in the output star coupler, as long as they do not physically overlap. Also, it is possible to add multiple input ports. This way, a $M \times N$ wavelength router can be built.[21]

3.3 Echelle Gratings

Echelle gratings operate in a similar way as AWGs, by combining a number of optical delays with a free-space imaging system.[22] The key difference with AWGs is that echelle gratings implement the delay lines as distances

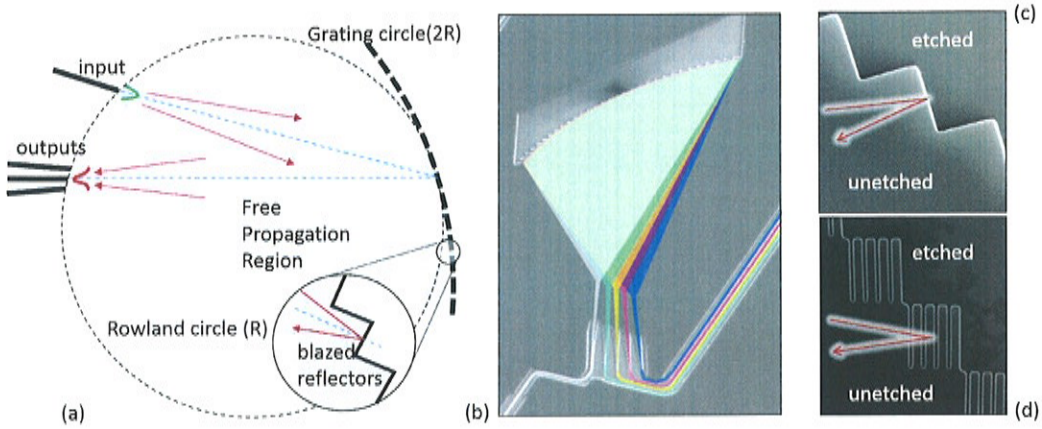

Figure 7. Echelle grating. (a) Basic design of the echelle grating, where the input and output apertures are located on the Rowland circle. (b) Fabricated echelle grating.[8] (c) Etched grating facets[22] and Bragg mirror grating facets.[23]

in the *free propagation region* set by the location of an array of reflecting facets. As shown in Fig. 7, the light traverses the same free propagation region twice. The exact phase delay is therfore not dependent on the linewidth of patterned waveguides, and this makes an echelle grating inherently more fabrication tolerant, because the optical delay length now depends only on the guiding layer, rather than on the exact geometry of a waveguide cross section. Still, thickness variations of the silicon layer can still introduce phase errors.

The fabrication-critical detail of echelle gratings are the reflector facets. Simply etched facets only have a reflection of 30-40%, which immediately introduces a 5dB insertion loss[22] . Better solutions involve the use of corner reflectors or distributed Bragg mirrors which can cut the reflection loss down to 1dB or less[23] . Just having a high reflection of the grating is not sufficient: it is important that the edges of the reflectors do not scatter too much light, because that gives rise to imaging errors and therefore distortion. So, while the image quality generally improves by using more reflectors (or grating elements), the reflectors should be sufficiently large to make sure the edge effects do not dominate the main body of the reflectors.

Like an AWG, an echelle grating can separate many wavelength channels into their own output waveguide, and they suffer from the same nonuniformity between channels as AWGs.

4. COMPARISON

We compare these different types of spectral filters to a number of criteria. The comparisons in this preliminary study are are a combination of simulations and fabricated devices, where we coupled the results of the fabrication back into the simulated models to predict the scaling trends of the different filters. With ideal technology, the different filter types can all exhibit a similar performance. However, when fabrication technology is imperfect, the performance will suffer; however, not for all filter types in the same way. Waveguide delay lines (MZI and AWG) will have different phase error statistics as delays implemented in the slab waveguide of an echelle grating. The control of directional couplers will impact Lattice filters much more than the two other filter types.

When the channel count within an FSR increases, this will have an affect on the performance as well. A large number of channels will require a larger number of delay lines (stages, arms, facets), and this in turn will increase the average delay length and phase error. As a result, the crosstalk and insertion loss will go up. We study both of these metrics by taking a fixed-channel filter design and vary the number of delays. We also compare how the different filter types scale in footprint when used as a wavelength channel demultiplexer. Even though silicon photonic devices are quite compact, (de)multiplexers with a large channel count can grow up to millimeters in size. Finally, we make a qualitative assessment on how the different technology aspects limit the scaling performance of the different filters.

4.1 Fabricated devices

We fabricated a set of MZI lattice filters, AWGs and echelle gratings using IMEC's passive silicon photonics platform. We varied the filters in channel spacing and number of channels, and characterized the devices on several dies on the same wafer using an automated probe station and vertical grating couplers.

From the transmission measurements we extracted the insertion loss, crosstalk, roll-off (ratio of 1dB bandwidth and 10dB bandwidth) and we calculated the footprint per channel. Table 1 lists a subset of this data for MZI lattice filters and AWGs. We can see several trends which are discussed in more detail using simulations based on the extracted parameters of these devices.

Table 1. Comparison of fabricated FIR filters in IMEC's silicon photonics platform.

	number of channels	FSR [nm]	IL [dB]	XT [dB]	1dB/10dB bandwidth ratio	footprint per channel [μm]
AWG	4	25.6	-1.36	-28	0.26	7800
	8	12.8	-1.24	-19	0.32	25800
	16	25.6	-1.55	-16	0.31	16800
MZI lattice	4	12.8	-0.66	-15.7	0.33	4300
(4 stages)	8	12.8	-1.08	-14.6	0.33	4300
MZI lattice	4	12.8	-0.40	-17.9	0.33	7800
(8 stages)	8	12.8	-0.55	-12.1	0.33	7800
MZI lattice	4	12.8	-0.77	-5.8	0.57	11200
(12 stages)	8	12.8	-2.72	-8.9	0.38	11300

One aspect which becomes clear in this table, is the minimum number of stages to obtain a box-like filter profile with an MZI lattice filter. We see that for all filters, the ration between 1dB bandwidth and 10dB bandwidth remains constant at approximately 0.33, which closely matches the roll-off of a Gaussian filter window. Only for the 12-stage, 4-channel filter we see a significant improvement of the roll-off. However, for this number of stages the other filter performance metrics, such as crosstalk, are already much worse.

Echelle gratings and AWGs are very similar in concept, and we have already published a comparison study between these two types of demultiplexers.[20] There it becomes clear that AWGs perform better for smaller channel spacings, while echelle gratings are the best choice for few channels with a large spacing. Some of the findings of this study has been included the results presented here.

4.2 Crosstalk

One of the most important performance metrics for wavelength filters is the crosstalk, i.e. the rejection of light with wavelengths outside the channel. For AWGs and echelle gratings, the crosstalk is entirely dependent on the quality of the image at the output apertures. That quality depends on the number of delays: more delays means a more detailed reconstruction of the input field profile. However, more delays will automatically imply a longer average delay length, and therefore higher phase errors. So for a small number of arms we expect a rapid decrease in crosstalk (better imaging) but then a gradual increase for large number of arms. We simulated this with different amounts of phase errors.

This is what we observe in Fig. 8. We see that for zero phase errors we do get a constant decline in crosstalk, but once we add phase errors we see that the crosstalk starts to increase from a certain number of arms. For MZI lattice filters the picture is a bit more complicated as the crosstalk is also very dependent on the control of coupling coefficients, so the absolute values of the crosstalk (which only take phase errors of waveguides into account) might be underestimated.

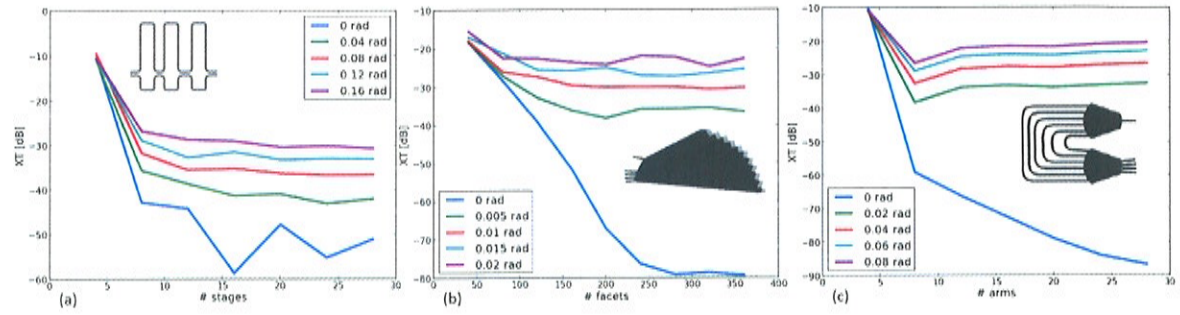

Figure 8. Scaling of crosstalk level of a 1:4 channel filter when increasing the number of delay lines. (a) MZI lattice filter, increasing the number of stages, (b) Echelle grating, inceasing the number of facets, and (c) AWG, increasing the number of arms.

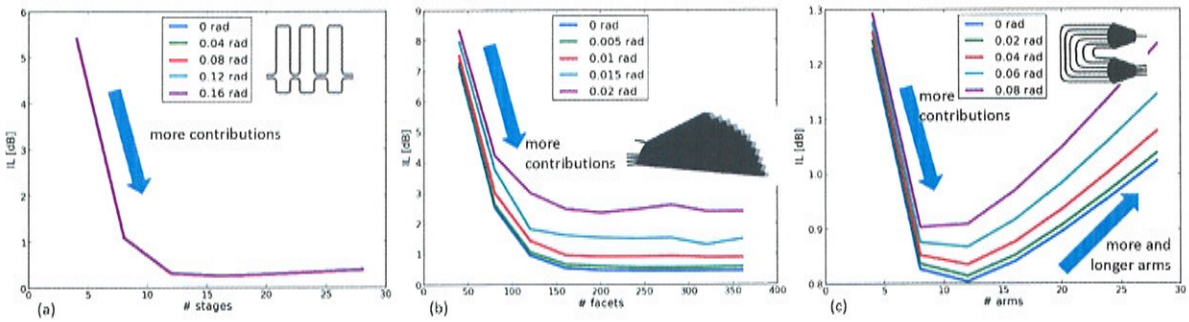

Figure 9. Scaling of crosstalk level of a 1:4 channel filter when increasing the number of delay lines. (a) MZI lattice filter, increasing the number of stages, (b) Echelle grating, inceasing the number of facets, and (c) AWG, increasing the number of arms.

4.3 Insertion Loss

For insertion loss we observe a similar pattern, which is understandable if one considers crosstalk as optical power which is not directed into the correct channel, and is therefore lost. The trends are plotted in Fig. 9. The most remarkable result is that of the MZI lattice filter, where the insertion loss is very independent of the phase errors. This is because we measured insertion loss as the maximum transmission within the wavelength channel. Phase errors do, however, impact the non-uniformity of the transmission within the channel band, and this starts to increase with larger phase errors.

4.4 Footprint

One of the metrics that have an impact on the filter choice is the actual footprint of the final device. Even though the different devices are based on the same principle, their implementation is very different, and this affects the chip area they consume. MZI lattice filters select a single channel (or act as an interleaver). When making a wavelength demultiplexer, the footprint of an MZI-based device therefore scales roughly with the $n.log(n)$, with n the number of channels: more channels within an FSR requires more MZI stages per channels, and to make a multiplexer of n channels we need between $log(n)$ and n filters, depending on the design of the demultiplexer as a cascaded or serial device. As the FSR gets smaller, smart layout of the longer MZI delays might still result in a compact design.

For AWGs, the footprint goes up with roughly the square of the channel number n: We need more delay lines, and the average delay line gets longer, and therefore consumes more space. When the FSR gets smaller,

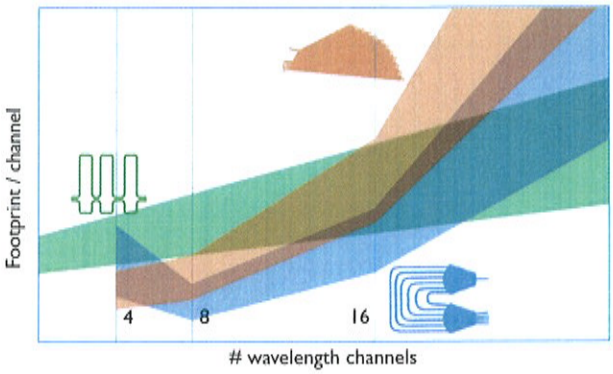

Figure 10. Relative scaling of filter footprint (per wavelength channel) for a demultiplexer, as function of the total number of channels within an FSR.

the device will scale inversely, and there are no straigthforward ways to reduce the footprint of the arrayed waveguides: folding the delay lines will result in additional phase errors.

The footprint of echelle gratings increases in a similar way as the AWGs. More and longer delays will increase the radius of the grating circle (for a constant spreading angle of the waveguide aperture). This will result in a quadratic increase of footprint as function of channel count n.

5. HOW TECHNOLOGY AFFECTS FILTER SCALING

The performance of the wavelength filters deteriorates with a larger number of channels (more delay lines) and a smaller FSR. However, as we have already seen, the different filter architectures scale in a different way for performance metrics such as crosstalk, insertion loss and footprint. Exactly how the performance scales depends heavily on the technology.

Fig. 11 shows how 6 technology parameters affect the crosstalk and insertion loss when scaling the number of channels and the FSR. We can see some clear trends there: arrayed waveguide gratings and MZI lattice filters are both strongly affected by the quality of the waveguides: absolute linewidth control, linewidth uniformity and waveguide loss. Naturally, echelle gratings are fairly impervious to the waveguide quality, but is on the other hand extremely sensitive to the thickness uniformity of the guiding layer. MZI lattice filters are very sensitive to the performance of directional couplers, so the technology should be able to control narrow gaps to a high precision. Both echelle gratings as AWGs require sufficiently small features, for the Bragg mirrors of the facets and the spacing of the apertures in the star coupler, respectively.

For many application, an important aspect of the performance of a filter bank, and especially a demultiplexer, is the absolute wavelength registration. This requires a control of the physical length as well as the effective index of the silicon waveguide. Given the sensitivity of silicon photonic waveguides, this is exceptionally hard. Again, we see the same sensitivities to linewidth control for the AWG and MZI lattice filter, while in the echelle grating we see a sensitivity to thickness control. However, for lattice filters, there are techniques to stabilize the wavelength of the filter, using different waveguides (or polarizations) in both arms,[24] and this reduces the overall sensitivity to fabrication errors. This technique could be extended to AWGs, which are also waveguide based, but would be difficult to implement for echelle gratings.

6. CONCLUSION

In this paper we presented a first discussion of a systematic study to compare silicon photonic wavelength filters. We compared non-resonat FIR filters: Mach-Zehnder lattice filters, arrayed waveguide gratings, and echelle gratings. We simulated the devices based on device properties extracted from fabricated devices and extracted scaling trends for crosstalk, insertion loss, and device footprint. We also assessed how different aspects of the fabrication technology affect the scaling of the filters in terms of channel count and channel spacing.

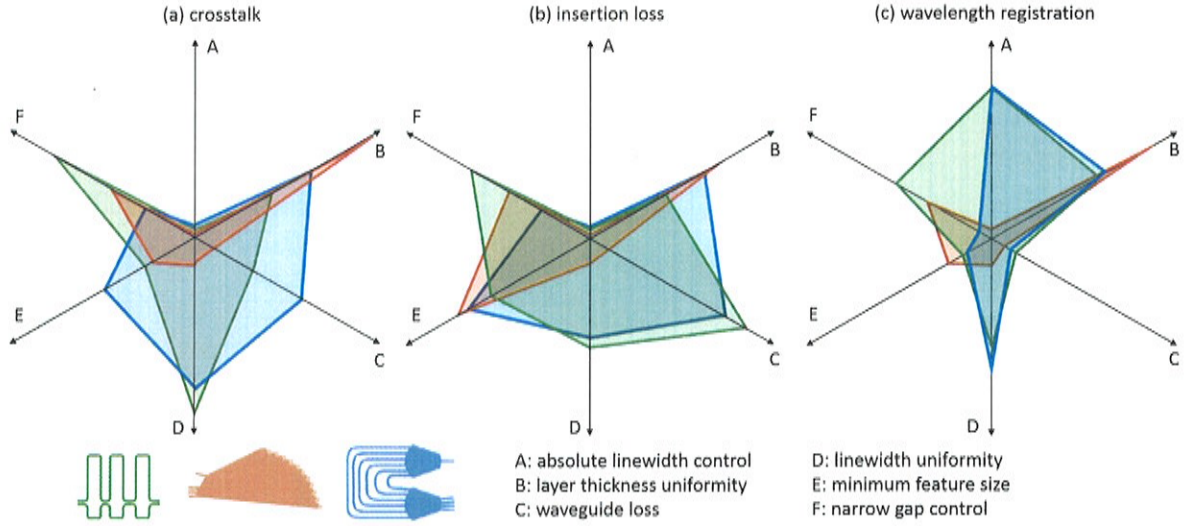

Figure 11. Impact of fabrication technology capability on the scaling performance of the different filters. The further outward, the more an aspect of the fabrication technology limits the scaling of the filter. (a) Crosstalk, (b) Insertion loss, and (c) wavelength accuracy.

ACKNOWLEDGEMENTS

All simulations were done using Luceda Photonics' IPKISS design tools and Caphe circuit simulator.

REFERENCES

[1] De Heyn, P., De Coster, J., Verheyen, P., Lepage, G., Pantouvaki, M., Absil, P., Bogaerts, W., Van Campenhout, J., and Van Thourhout, D., "Fabrication-tolerant four-channel wavelength-division-multiplexingfilter based on collectively tuned si microrings," *J. Lightwave Technol.* **31**, 3085–3092 (Aug 2013).

[2] Claes, T., Bogaerts, W., and Bienstman, P., "Experimental characterization of a silicon photonic biosensor consisting of two cascaded ring resonators based on the vernier-effect and introduction of a curve fitting method for an improved detection limit," *Optics Express* **18**(22), 22747–22761 (2010).

[3] Trita, A., Vickers, G., Mayordomo, I., van Thourhout, D., and Vermeiren, J., "Design, integration, and testing of a compact FBG interrogator, based on an awg spectrometer," (2014).

[4] Chen, L., Li, J., Spasojevic, M., and Adams, R., "Nanowires and sidewall bragg gratings in silicon as enabling technologies for microwave photonic filters," *Opt. Express* **21**, 19624–19633 (Aug 2013).

[5] Narasimha, A., Analui, B., Liang, Y., Sleboda, T., Abdalla, S., Balmater, E., Gloeckner, S., Guckenberger, D., Harrison, M., Koumans, R., Kucharski, D., Mekis, A., Mirsaidi, S., Song, D., and Pinguet, T., "A fully integrated 4 times; 10-gb/s dwdm optoelectronic transceiver implemented in a standard 0.13 m cmos soi technology," *Solid-State Circuits, IEEE Journal of* **42**, 2736–2744 (Dec 2007).

[6] Mekis, A., Gloeckner, S., Masini, G., Narasimha, A., Pinguet, T., Sahni, S., and De Dobbelaere, P., "A Grating-Coupler-Enabled CMOS Photonics Platform," *IEEE J. Sel. Top. Quantum Electron.* **17**, 597–608 (May-Jun. 2011).

[7] Verheyen, P., Pantouvaki, M., Van Campenhout, J., Absil, P. P., Chen, H., De Heyn, P., Lepage, G., De Coster, J., Dumon, P., Masood, A., and Bogaerts, W., "Highly uniform 25 Gb/s Si photonics platform for high-density, low-power wdm optical interconnects," in [*Integrated Photonics Research, Silicon and Nanophotonics*], IW3A–4 (2014).

[8] Bogaerts, W., Selvaraja, S., Dumon, P., Brouckaert, J., De Vos, K., Van Thourhout, D., and Baets, R., "Silicon-on-insulator spectral filters fabricated with cmos technology," *J. Sel. Top. Quantum Electron.* **16**(1), 33–44 (2010).

[9] Yamada, K., Shoji, T., Tsuchizawa, T., Watanabe, T., Takahashi, J., and Itabashi, S., "Silicon-wire-based ultrasmall lattice filters with wide free spectral ranges," *J. Sel. Topics Quantum Electron* **11**, 232–240 (2005).

[10] Horst, F., Green, W., Assefa, S., Shank, S., Vlasov, Y., and Offrein, B., "Cascaded mach-zehnder wavelength filters in silicon photonics for low loss and flat pass-band wdm (de-)multiplexing," *Opt. Express* **21**, 11652–11658 (May 2013).

[11] Bogaerts, W., De Heyn, P., Van Vaerenbergh, T., De Vos, K., Kumar Selvaraja, S., Claes, T., Dumon, P., Bienstman, P., Van Thourhout, D., and Baets, R., "Silicon microring resonators," *Laser Photon. Rev.* **6**(1), 47–73 (2012).

[12] Dulkeith, E., Xia, F., Schares, L., Green, W., and Vlasov, Y., "Group index and group velocity dispersion in silicon-on-insulator photonic wires," *Opt. Express* **14**, 3853–3863 (May 2006).

[13] Goh, T., Suzuki, S., and Sugita, A., "Estimation of waveguide phase error in silica-based waveguides," *J. Lightwave Technol.* **15**(11), 2107–2113 (1997).

[14] Suzuki, S., Inoue, Y., and Kominato, T., "High-density integrated 1 × 16 optical fdm multi/demultiplexer," in [*Lasers and Electro-Optics Society Annual Meeting, 1994. LEOS '94 Conference Proceedings. IEEE*], **2**, 263–264 vol.2 (Oct 1994).

[15] Dragone, C., "An NxN optical multiplexer using a planar arrangement of two star couplers," *IEEE Photon. Technol. Lett.* **3**, 812–814 (Sept. 1991).

[16] Soole, J. B. D., Amersfoort, M., Leblanc, H., Andreadakis, N. C., Rajhel, A., Caneau, C., Bhat, R., Koza, M., Youtsey, C., and Adesida, I., "Use of multimode interference couplers to broaden the passband of wavelength-dispersive integrated wdm filters," *Photon. Technol. Lett.*, **8**(10), 1340–1342 (1996).

[17] Dragone, C., "Efficient techniques for widening the passband of a wavelength router," *J. Lightwave Technol.* **16**, 1895–1906 (oct 1998).

[18] Pathak, S., Vanslembrouck, M., Dumon, P., Van Thourhout, D., and Bogaerts, W., "Optimized silicon awg with flattened spectral response using an mmi aperture," *J. Lightwave Technol.* **31**(1), 87–93 (2013).

[19] Spuesens, T., Pathak, S., Vanslembrouck, M., Dumon, P., and Bogaerts, W., "Integrated grating coupler/power splitter for on-chip optical power distribution," in [*Group IV Photonics (GFP), 2014 IEEE 11th International Conference on*], 141–142, IEEE (2014).

[20] Pathak, S., Dumon, P., Van Thourhout, D., and Bogaerts, W., "Comparison of awgs and echelle gratings for wavelength division multiplexing on silicon-on-insulator," *Photonics Journal, IEEE* **6**, 1–9 (Oct 2014).

[21] Dumon, P., Bogaerts, W., Van Thourhout, D., Taillaert, D., Baets, R., Wouters, J., Beckx, S., and Jaenen, P., "Compact wavelength router based on a silicon-on-insulator arrayed waveguide grating pigtailed to a fiber array," *Opt. Express* **14**, 664–669 (January 2006).

[22] Brouckaert, J., Bogaerts, W., Dumon, P., Van Thourhout, D., and Baets, R., "Planar concave grating demultiplexer fabricated on a nanophotonic silicon-on-insulator platform," *J. Lightwave Technol.* **25**(5), 1269–1275 (2007).

[23] Brouckaert, J., Bogaerts, W., Selvaraja, S., Dumon, P., Baets, R., and Van Thourhout, D., "Planar concave grating demultiplexer with high reflective bragg reflector facets," *IEEE Photon. Technol. Lett.* **20**(4), 309–311 (2008).

[24] Dwivedi, S., D'heer, H., and Bogaerts, W., "A compact all-silicon temperature insensitive filter for WDM and bio-sensing applications," *IEEE Photon. Technol. Lett.* **25**(22), 2167–2170 (2013).

Proceedings Article

Silicon photonics non-resonant wavelength filters: comparison between AWGs, echelle gratings, and cascaded Mach-Zehnder filters

Wim Bogaerts ; Shibnath Pathak ; Alfonso Ruocco ; Sarvagya Dwivedi

[+] Author Affiliations

Proc. SPIE 9365, Integrated Optics: Devices, Materials, and Technologies XIX, 93650H (April 2, 2015); doi:10.1117/12.2082785

From Conference Volume 9365

Integrated Optics: Devices, Materials, and Technologies XIX
Jean-Emmanuel Broquin; Gualtiero Nunzi Conti
San Francisco, California, United States | February 07, 2015

abstract

We present a comparison of different silicon photonics-based wavelength filters for different design criteria (e.g. channel spacing, number of channels, ...) and different performance metrics (e.g. insertion loss or crosstalk). In this paper we compare only non-resonant filters, or finite-impulse response (FIR) filters, such as Arrayed Waveguide Gratings, Echelle Gratings and higher-order cascades of Mach-Zehnder filters. We derive the strengths and weaknesses from their operational principles and confirm those with experimental data from fabricated devices and extrapolated simulations.

Topics

Interference (communication) ; Photonics ; Silicon ; Silicon photonics ; Simulations ; Waveguides

Citation Wim Bogaerts ; Shibnath Pathak ; Alfonso Ruocco and Sarvagya Dwivedi " Silicon photonics non-resonant wavelength filters: comparison between AWGs, echelle gratings, and cascaded Mach-Zehnder filters ", *Proc. SPIE* 9365, Integrated Optics: Devices, Materials, and Technologies XIX, 93650H (April 2, 2015); doi:10.1117/12.2082785; http://dx.doi.org/10.1117/12.2082785